Bioinorganic and Medicinal Inorganic Chemistry Journal

# Biomolecule (RNA) binding analysis of [$SnMe_2Cl_2(Me_2phen)$] complex: multi-spectroscopic analysis and docking simulation

**Nahid Shahabadi[a*], Saba Zendehcheshm[a], Badri Z Momeni[b], Fatemeh Khademi[c]**

[a] Inorganic Chemistry Department, Faculty of Chemistry, Razi University, Kermanshah, Iran

[b] Department of Inorganic Chemistry, Faculty of Chemistry, K.N. Toosi University of Technology, Tehran, Iran

[c]Medical Biology Research Center, Health Technology Institute, Kermanshah University of Medical Sciences, Kermanshah, Iran

*****Correspondence: Nahid Shahabadi, Faculty of Chemistry, Razi University, Kermanshah, IRAN

Tel / Fax: +98-8334274559

E-mail: nahidshahabadi@yahoo.com

*Received: 12 March 2023*

*revised: 17 March 2023*

*Accepted: 19 March 2023*

*Available online: 19 March 2023*

*DOI: 10.22126/BMCJ.2023.2572*



**Abstract:** In this study, the spectroscopic methods (UV–vis and fluorometric), and computational study (molecular docking) were used to investigate the interaction of [$SnMe_2Cl_2(Me_2phen)$] complex with RNA under simulative physiological conditions (pH =7.40). The RNA binding properties of the Sn(IV) complex exhibit that it binds to RNA through a groove binding mode and the binding constant values were computed employing the emission spectral data. The values of $K_a$ from fluorescence measurement clearly underscore the high affinity of [$SnMe_2Cl_2(Me_2phen)$] complex to RNA. The experimental results of fluorescence showed that the quenching of the complex by RNA is static. The thermodynamic parameters ($\Delta H^0 > 0$ and $\Delta S^0 > 0$) are calculated by van't Hoff equation, which demonstrated that hydrophobic interactions played major roles in the binding reaction. In this context, a negative free energy change ($\Delta G^0 < 0$) emphasizes the spontaneity of the binding process. In silico molecular docking studies further corroborated well with the experimental results.

**Keywords:** RNA; Sn(IV) complex; Thermodynamic parameters; Molecular docking; Interaction

## 1. Introduction

Organotin complexes are species that have at least one carbon-tin bond in their structure. Organometallic complexes have various usages such as catalyst in trans esterification of vegetable oil into biodiesel, wood preservatives, marine antiseptic agents, silicon curing, formation of polyurethane, antifouling paints, stabilizers in polymers and so forth [1-7]. Through their structural versatility and broad therapeutic activity, they get a lot of attention in the field of medical chemistry. The therapeutic activity of organotin compounds is due to their molecular geometry, ease of hydrolysis of ligands and accessibility of coordination position around central tin atom [8]. They have many different activities similar to antiparasitic [9], anti-HIV [10], antimicrobial, antiallergic [11, 12], antitumor [13-19], anti-inflammatory [20-22] and in agriculture as bactericidal, acraricidal and fungicidal agents [23, 24]. Most effects show that organotin compounds have anti-proliferative effects against the solid and hematologic cancers [25] and they also exhibit potential

antineoplastic [26, 27] and antituberculosis activities [28, 29]. Studies of the interaction between metal complexes and nucleic acids (DNA and RNA) in terms of understanding of how to target nucleic acids sites with specificity may lead to developing highly sensitive chemotherapeutic agents [30]. The nucleic acids binding of the transition metal complexes has been studied since these complexes bear potential applications in bioinorganic chemistry [31]. The interaction of metal complexes with biological macromolecules such as nucleic acids is a crucial pharmacological phenomenon in biosciences therefore, it has invoked great attention in recent decades [32]. The therapeutic potential of a drug depends upon the degree and mode of interaction with nucleic acids as these interactions play an imperative role in understanding the mechanism of binding and the forces involved in it [33]. Molecular interactions can affect the structure, distribution, physiological action and elimination of drugs and thereby influence the therapeutic efficacy of the drug [34, 35]. Nucleic acids (DNA & RNA) participate in a variety of biological processes [36, 37] such as gene storage, replication, transcription and other important biological activities and also play significant roles in anticancer [38] and antiviral [39] processes. Therefore, targeting nucleic acids can be desirable for drug design [40]. Numerous studies reveal that DNA is the primary intracellular target of antitumor drugs, because the interaction between small molecules and DNA can lead to alteration in DNA replication or blocking DNA synthesis in cancerous cells, eventually inhibiting the growth of cancerous cells. Therefore, the metal complexes which can efficiently bind and cleave DNA are considered as promising candidates for use as therapeutic agents [41-43]. However, RNA target is still under rated as compared to DNA. Nevertheless, researchers have realized recently that RNA, the chemical cousin of DNA can be exploited as a better drug target over DNA because of its unique structural polymorphism [44], absence of the cellular repair mechanism, [45] and its ability to fold into intricate three dimensional (3D) secondary and tertiary structures which provides recognition domains leading to their higher binding affinity and specificity with small molecules [46]. In our recent research, we reported the interaction of [$SnMe_2Cl_2(Me_2phen)$] complex with DNA through Multi-spectroscopic analysis, atomic force microscopy, molecular docking and molecular dynamic simulation studies [47]. In continuation of our previous research, herein, the interaction of [$SnMe_2Cl_2(Me_2phen)$] complex with RNA was studied using spectroscopic and docking simulation methods to evaluate the RNA-[$SnMe_2Cl_2(Me_2phen)$] binding propensity. Studies on the interaction model and the mechanism between [$SnMe_2Cl_2(Me_2phen)$] complex and biological molecules such as RNA have not yet been fully and systematically studied. To gain insight into the interaction model and the mechanism, investigating the interaction of [$SnMe_2Cl_2(Me_2phen)$] complex with RNA is necessary. In similar work, Parveen et al. [48] reported the interaction of enantiomeric Cu(II) complexes with DNA, RNA and HSA. Bandyopadhyay et al. [49] showed biophysical studies on the interaction of a novel oxime-based palladium (II) complex with DNA and RNA.

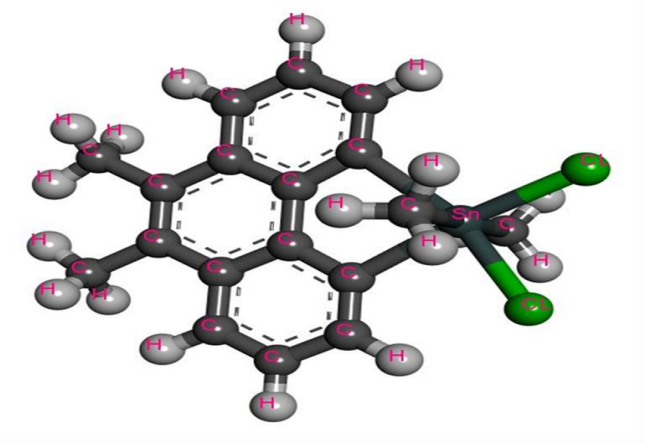

**Figure 1 The chemical structure of [$SnMe_2Cl_2(Me_2phen)$] complex.**

## *2. Materials and methods*

### *2.1. Apparatus*

An Agilent 8453 spectrophotometer with a 1.00 cm quartz cell was utilized to perform the UV–vis spectroscopic measurement of RNA-complex systems. A JASCO FP 6200 spectrofluorometer with a quartz cuvette of 1.00 cm path length was employed to measure the emission spectra. A Metrohm model of 827 pH meters was utilized to evaluate the pH values.

### *2.2. Materials*

The Tris- (hydroxymethyl)-amino-methane–hydrogen chloride, Baker's yeast RNA, for RNA interaction were purchased from Sigma Aldrich and Merck Millipore. All stock solutions were prepared by employing a Tris-HCl buffer. The Tris-HCl buffer solution (pH= 7.4) was prepared by dissolving the Tris–(hydroxymethyl)-amino-methane in double distilled water. Approximately 3 mg of RNA powder was dissolved in 3 mL Tris–HCl buffer (10 mM) to prepare the stock solution of RNA. The purity of RNA was tested to meet the experimental requirements ($A_{260}/A_{280}$ > 1.8) [50]. The [$SnMe_2Cl_2(Me_2Phen)$] complex (Figure 1) has been synthesized according to the method characterized in the literature [51]. Due to the solubility of the complex in the water, a stock solution ($1.00 \times 10^{-3}$ M) was prepared by dissolving the compound in doubly distilled water.

### *2.3. RNA interaction of [$SnMe_2Cl_2(Me_2phen)$] complex*

#### *2.3.1. UV–vis spectroscopy*

The absorption signals of [complex + RNA] − [RNA] were noted in Tris-HCl buffer solution in the range of 200-350 nm.

During the interaction process, the concentration of the complex was maintained ($3.4\times10^{-5}$M), while the RNA concentration was varied (from $2.64\times10^{-5}$ to $3.70\times10^{-4}$ M).

### *2.3.2. Fluorescence studies*

The emission spectra of the complex were excited at 270 nm and scanned from 280 to 500 nm. The measurements were performed by maintaining the concentration of the complex constant ($1.00 \times 10^{-6}$ M) while changing the RNA concentration from $2.73\times10^{-5}$ to $2.62\times10^{-4}$ M at different temperatures (288.15, 298.15, and 310.15 K). In order to obtain the applicable data, fluorescence intensity values must be corrected for eliminating the inner filter effect.

$$F_{cor}=F_{obs}\times e^{(Aex+ Aem)/2} \quad (1)$$

Where $F_{obs}$ and $F_{cor}$ are observed and corrected fluorescence intensity, $A_{em}$, and $A_{ex}$ are the absorbance values for emission, and excitation wavelengths, respectively [52].

### *Evaluating association mode*

In order to investigate the mode of RNA - complex interaction, an intercalator fluorescence probe (EB) and groove binders (Hoechst 33258) were used. The displacement experiment was carried out to elucidate the potential of the complex to displace probes from the RNA structure. At first, the RNA ($2.73\times10^{-5}$ M) was added to the EB, and Hoechst ($5.00\times10^{-6}$ M) solutions. Then, this mixture was titrated with various concentrations of the complex ($8.00\times10^{-7}$ to $1.18\times10^{-5}$ M). The RNA-probes systems were excited at 526 nm, and 340 nm for EB, and Hoechst, respectively. Meanwhile, the scanning range of emission spectra between 530–720 nm, and 350–650 nm was set for EB, and Hoechst, respectively.

### 2.3.3. Molecular docking study

The molecular docking study of the interaction between the Sn(IV) complex with RNA was performed using Open-source AutoDock Vina (version 1.5.7) with MGL tools 1.5.4 [53]. We provided the three-dimensional structure of yeast RNA (PDB ID: 6TNA) from the Protein Data Bank and employed AutoDock Tools to confect the receptor and 'the ligand' files. The RNA was enclosed in a 60 × 36 ×86 box directions and grid set centers of 29.25, 17.55, and 47.29 Å with a grid spacing of 1.00 Å.

## *3. Results and discussion*

### *3.1. The interaction of [$SnMe_2Cl_2(Me_2phen)$] complex with RNA:*

#### *3.1.1 UV-vis absorption spectroscopy*

The absorption spectral measurements are one of the effective tools for estimating the association of [$SnMe_2Cl_2(Me_2phen)$] complex with biomacromolecules like RNA through monitoring the alteration in the spectral properties of biomacromolecules like the red shift or blue shift of the peak position and the hypochromic or hyperchromic effect of the peak intensity [54]. The UV-visible spectra of the Sn(IV) complex in the absence and presence of an elevating concentration of RNA are depicted in Figure 2. With the increasing concentration of RNA, there was a progressive increase in the absorption in the range from 240 to 290 nm. In general, hyperchromism has been linked to the presence of various non-covalent interactions. These interactions may include electrostatic binding, hydrogen bonding, and groove binding [55]. Also, two isosbestic points indicat the formation of a new [$SnMe_2Cl_2(Me_2phen)$] -RNA complex and show that the binding of [$SnMe_2Cl_2(Me_2phen)$] to RNA indeed exists [56]. Further experiments were performed to study the binding mode in more detail.

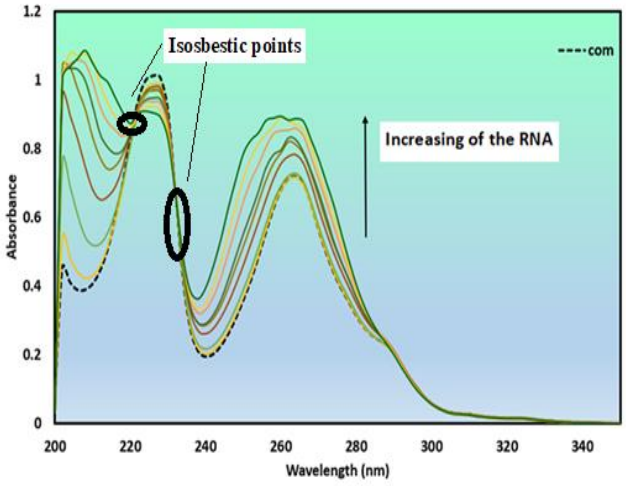


**Figure 2 Uv-vis spectra of Sn(IV) complex in the absence and presence of increasing amounts of RNA. ([Sn(IV) complex] =$3.40\times10^{-5}$ M, [RNA] = $2.64\times10^{-5}$ to $3.71\times10^{-4}$ M).**

#### *3.1.2 Fluorescence quenching titrations*

The interactions of RNA molecule with the Sn(IV) complex were further studied by fluorescence method. Figure. 3 shows that the complex exhibited a strong emission maximum at 371 nm after excitation at 270 nm. This figure indicates a decrease in the fluorescence intensity of the Sn(IV) complex with increasing concentration of RNA.

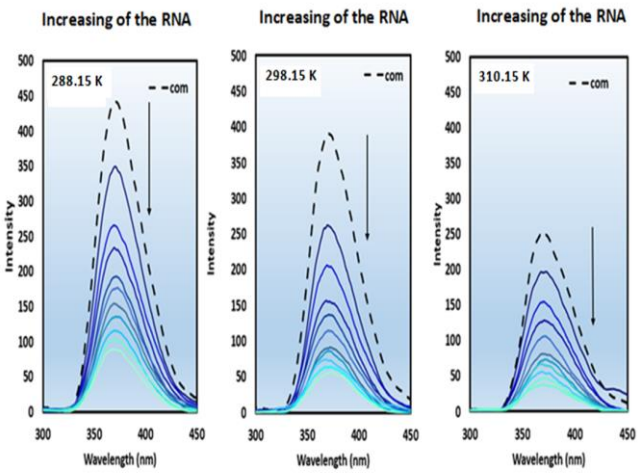


**Figure 3 Fluorescence emission spectra of Sn(IV) complex in the presence of the RNA at three temperatures (288.15, 298.15, and 310.15 K).([Sn(IV) complex]= $1.00\times10^{-6}$ M, [RNA]= $2.73\times10^{-5}$ to $2.62\times10^{-4}$ M).**

The Stern-Volmer equation was utilized to describe the fluorescence quenching mechanism:

$$F_0/F = 1 + K_q\,\tau_0\,[Q] = 1 + K_{sv}\,[Q] \qquad (2)$$

In the mentioned equation $F_0$ is the fluorescence intensity of the Sn(IV) complex in the absence of quencher (RNA), F is the fluorescence intensity of the Sn(IV) complex in the presence of RNA as a quencher, $K_{sv}$ is the Stern–Volmer constant and [Q] is the concentration of RNA, respectively.

The quenching constant of Stern–Volmer ($K_{sv}$) was obtained from the slope of the plot of $F_0/F$ vs [RNA] (Figure. 4). The limiting diffusion rate constant of the biomolecule is known to be around $2.0 \times 10^{10}$ $M^{-1}S^{-1}$, thus if the value of $K_q$ is higher than the limiting diffusion rate constant, the quenching process is static rather than dynamic [57]. In this work, the Stern–Volmer plot is linear, indicating that only one type of quenching process occurs, either static or dynamic quenching [58]. The results in Table 1 indicate that $K_{sv}$ has been increased with increasing temperature (dynamic quenching) and $K_q$ is higher than the limiting diffusion rate constant (static quenching) [59]. These two kinds of quenching mechanisms demonstrate some differences that can be distinguished experimentally, such as the change in the UV–Vis spectra. The dynamic quenching only affects the excited state of the quenching molecule with no function on the absorption spectrum of quenching substances, whereas a complex of RNA and ligand forms in static quenching, so there will be some changes in the UV–Vis spectra of the ligand. Thus, we employed UV–Vis absorption spectra to give some more evidence for the actual quenching process. The UV–Vis absorption spectra of the Sn(IV) complex in the absence and presence of RNA were measured (Figure.2). According to the UV–Vis spectra, the fluorescence quenching of the Sn(IV) complex by RNA seems to be primarily caused by complex formation between the Sn(IV) complex and RNA (i.e., static quenching).

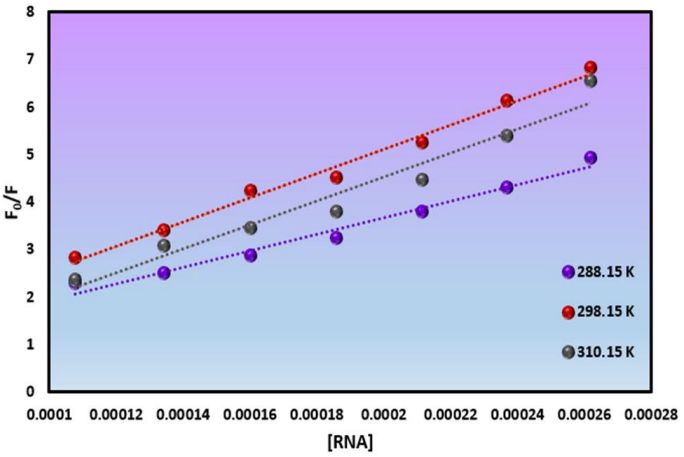


**Figure 4 Plot of $F_0/F$ versus [RNA] for RNA– Sn(IV) complex system.**

The number of binding sites (n) and the values of the association constant ($K_a$) for [$SnMe_2Cl_2(Me_2phen)$] -RNA interaction were estimated according to the equation given below:

$$\log [(F_0 - F)/F] = \log K_a + n \log [Q] \qquad (3)$$

The values of n and $K_a$ could be determined from the intercept and slope of linear regression of log $(F_0 - F)/F$ versus log [Q] (Figure.5). The corresponding results of the binding constant and n are listed in Table 1. The values of n are approximately equal to 1 suggesting that there is only one kind of binding site available on RNA for [$SnMe_2Cl_2(Me_2phen)$]. The increase in the values of $K_a$ rise in temperature suggests that the [$SnMe_2Cl_2(Me_2phen)$] – RNA complex increases its stability with rising temperature [60].

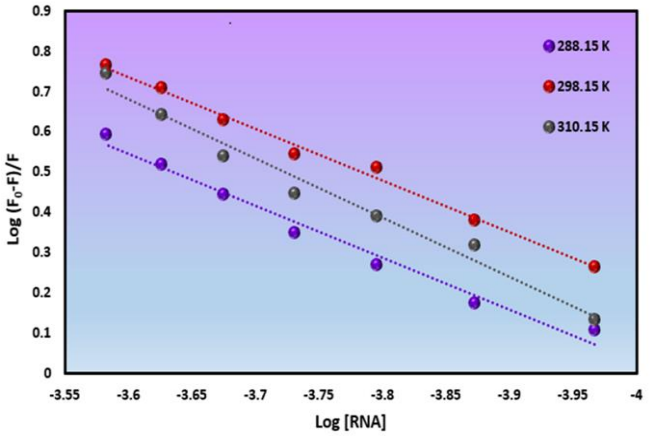


**Figure 5 Plot of log $(F_0-F)/F$ versus log [RNA] for RNA – Sn(IV) complex system.**

### *Thermodynamic Parameters and Interaction Forces*

The thermodynamic parameters for binding were calculated from the temperature dependence of the binding constant to deduce the type of binding interactions (van der Waals, hydrogen bonding, electrostatic, and the hydrophobic) between [$SnMe_2Cl_2(Me_2phen)$] and RNA. The van't Hoff equation (Equation (4)) was utilized to determine the $\Delta H^0$ and $\Delta S^0$ by employing the values of $K_a$ at three different temperatures.

$$\text{Ln } K_a = -\Delta H^0/RT + \Delta S^0/R \qquad (4)$$

The slope and intercept of the Van't Hoff equation were employed to compute the binding enthalpy and binding entropy of the complex – RNA system.

The free energy change ($\Delta G^0$) was then estimated from the following relationship:

$$\Delta G^0 = \Delta H^0 - T\Delta S^0 \qquad (5)$$

The sign of $\Delta G^0$ is negative, which indicated that the interaction between [$SnMe_2Cl_2(Me_2phen)$] and RNA was spontaneous. The positive values of enthalpy and entropy acquired from the interaction of RNA with the Sn(IV) complex indicate that hydrophobic interactions are the main forces of RNA -[$SnMe_2Cl_2(Me_2phen)$] complex formation [61].

**Table 1 Thermodynamic and binding parameters of the interaction of the Sn(IV) complex to RNA.**

| T(K) | $K_{sv}(M^{-1})$ | $K_q(M^{-1}S^{-1})$ | $K_r(M^{-1})$ | $R^2$ | n | $\Delta G^0(kJmol^{-1})$ | $\Delta H^0(kJmol^{-1})$ | $\Delta S^0(Jmol^{-1}K^{-1})$ |
|---|---|---|---|---|---|---|---|---|
| 288.15 | $1.73\times10^4$ | $1.73\times10^{12}$ | $6.16\times10^4$ | 0.99 | 1.18 | -25.63 | 91.36 | 406.00 |
| 298.15 | $2.46\times10^4$ | $2.46\times10^{12}$ | $8.51\times10^4$ | 0.99 | 1.17 | -29.69 | | |
| 310.15 | $2.53\times10^4$ | $2.53\times10^{12}$ | $8.91\times10^5$ | 0.98 | 1.46 | -34.56 | | |

### *Dye displacement assays with Hoechst 33258 and EB*

To determine the mode of binding to RNA, competitive binding experiments were performed. EB as classical intercalators and Hoechst 33258 as groove binder probes were used respectively, to clarify the nature of the interaction between the Sn(IV) complex and RNA [62]. The complex was added to the RNA-Hoechst 33258, and RNA-EB system, and the fluorescence intensity was recorded to enhance the concentrations of the complex. As can be seen, the addition of the complex has no effect on the emission intensity of the RNA-EB system Figure. 6B. However, the fluorescence intensity of RNA - Hoechst system is decreased (quenched) on enhancing the concentration of the complex Figure. 6A. meanwhile, we can mention that the complex was bound to RNA and avoided Hoechst binding. These experimental results clearly exposed that the binding mode of the complex - RNA was groove [63].

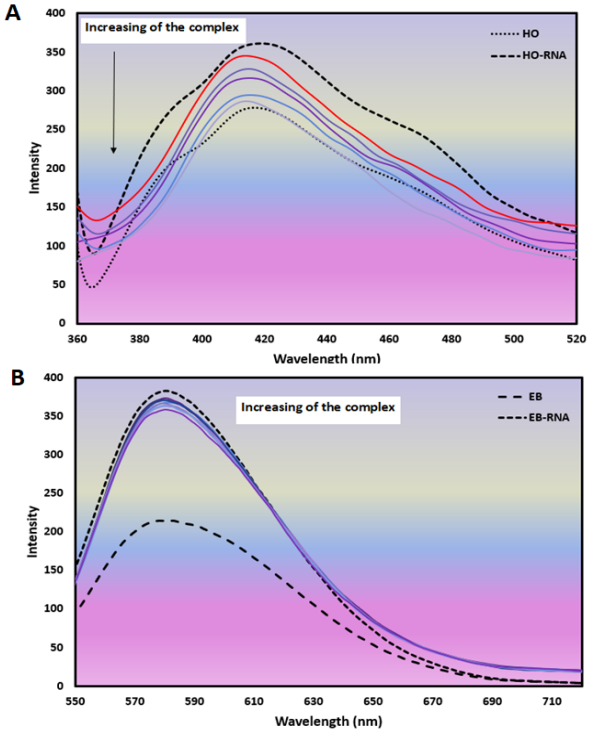


**Figure 6 Fluorescence spectra of (A) Hoechst + RNA, (B) EB+ RNA in the presence of Sn(IV) complex ($8.00\times10^{-7}$ to $1.18\times10^{-5}$ M), RNA= ($2.73\times10^{-5}$ M) $C_{\text{Hoechst, EB}}$ =($5.00\times10^{-6}$ M).**

### *3.1.3. Docking simulation*

Docking simulation is a fundamental method to evaluate the interaction of RNA with metal complexes on atomic level. Furthermore, the docking studies were also performed towards the molecular target, yeast RNA (PDB ID: 6TNA) to determine the specific recognition sites on RNA. Yeast RNA possesses well-defined 3D structures having regions like T arm, D arm, Ψ loop, anticodon arm and acceptor stem [64]. These structural motifs are involved directly or indirectly with the complexes binding to the specific targets. Appling Gaussian 03 W suite of programs the starting geometry of Sn(IV) complex was optimized through the density functional theory (DFT)//B3LYP/LanL2DZ level to make all eigenvalues of the Hessian matrix positive [65]. The docked pose model suggested that the complex fitted into the active pocket located between the upper and lower stem and was in close proximity to U6 and U7. This resulting model exhibited intermolecular hydrophobic between U6 and U7of RNA and C atoms of the complex (Figure. 7) (Table 2). There is a good agreement between run 1 with the best rmsd of 0.00 u.b and our experimental results. Meanwhile, the best-reported value of ΔG (-32.22 kJ/mol) in 20 orientations is in correlation with the fluorescence experiments (-34.56 kJ/mol).

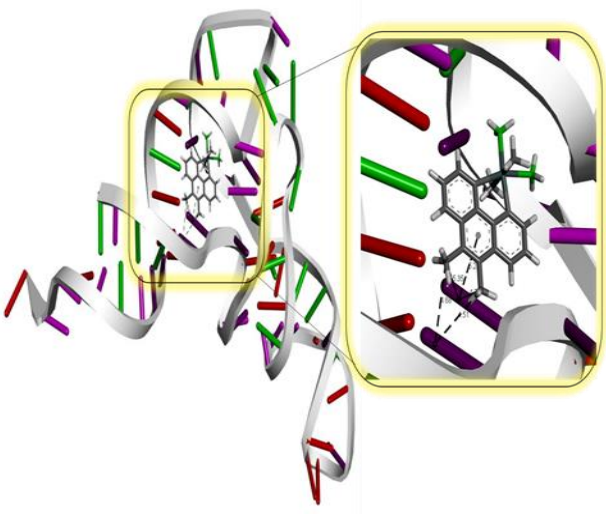

**Figure 7 Molecular docking of Sn(IV) complex to the RNA.**

**Table2. Predicted bonds between interacting atoms of the nucleotides of RNA [PDB ID: 6TNA] and Sn(IV) complex.**

| S. No. | RNA strand | Nucleotide | Sn(IV) complex atom | Distance (A°) | Nature of interaction |
|---|---|---|---|---|---|
| 1 | A | U7 (Pi-Orbitals) | Pi-Orbitals | 5.23 | Hydrophobic (Pi-Pi T-shaped) |
| 2 | A | U6 (Pi-Orbitals) | C (Alkyl) | 4.68 | Hydrophobic (Pi-Alkyl) |
| 3 | A | U6 (Pi-Orbitals) | C (Alkyl) | 4.51 | Hydrophobic (Pi-Alkyl) |
| 4 | A | U7 (Pi-Orbitals) | C (Alkyl) | 5.35 | Hydrophobic (Pi-Alkyl) |
| 5 | A | U7 (Pi-Orbitals) | C (Alkyl) | 4.70 | Hydrophobic (Pi-Alkyl) |

## *Conclusion*

Employing a biomacromolecule (viz; RNA), we have deciphered into the binding affinity and molecular recognition process of [SnMe2Cl2(Me2phen)] complex using multispectroscopic and computational methods (molecular docking). The experimental results of fluorescence showed that the quenching of the complex by RNA is static. The received data represented that the interaction mode between the complex and RNA is resulting from a groove binding mode. Competitive binding studies with Hoechst-RNA represented the ability of the complex to displace Hoechst from the Hoechst-RNA system, confirming the groove binding mode between the complex and RNA. Finally, we believe that the binding mode of [SnMe2Cl2(Me2phen)] complex with RNA studied here will provide useful information on the mechanism of drug binding to RNA and thus will be very helpful to the design of new drugs with low toxicity.

## *Acknowledgment*

The authors thank the Razi University Research Council for support of this work

## *References*

[1] A.V. Ivanov, E. Korneeva, A. Gerasimenko, W. Forsling, Structural organization of nickel (II), zinc (II), and copper (II) complexes with diisobutyldithiocarbamate: EPR, 13 C and 15 N CP/MAS NMR, and X-ray diffraction studies, Russian Journal of Coordination Chemistry 31 (2005) 695-707.

[2] I. Omae, Organotin antifouling paints and their alternatives, Applied organometallic chemistry 17.2 (2003) 81-105.

[3] D. Park, J.A. Finlay, R.J. Ward, C.J. Weinman, S. Krishnan, M. Paik, K.E. Sohn, M.E. Callow, J.A. Callow, C.L. Willis, Antimicrobial behavior of semifluorinated-quaternized triblock copolymers against airborne and marine microorganisms, ACS Applied Materials & Interfaces 2.3 (2010) 703-711.

[4] E.R. Tiekink, Tin dithiocarbamates: applications and structures, 9 (2008) 533-550.

[5] F.W. Sunderman, Nasal toxicity, carcinogenicity, and olfactory uptake of metals, Annals of Clinical & Laboratory Science 31.1 (2001) 3-24.

[6] D.L. Bodenner, P.C. Dedon, P.C. Keng, R.F. Borch, Effect of diethyldithiocarbamate on cis-diamminedichloroplatinum (II)-induced cytotoxicity, DNA cross-linking, and γ-glutamyl transpeptidase inhibition, Cancer research. 46 (1986) 2745-2750.

[7] B. Radke, M. Staniszewska, A. Wasik, J. Namieśnik, J. Bolałek, Organotin Compounds in Marine Sediments, Polish Journal of Environmental Studies 17.5 (2008).

[8] F. Barbieri, M. Viale, F. Sparatore, G. Schettini, A. Favre, C. Bruzzo, F. Novelli, A. Alama, Antitumor activity of a new orally active organotin compound: a preliminary study in murine tumor models, Anti-cancer drugs 13.6 (2002) 599-604.

[9] D. Kovala-Demertzi, V. Dokorou, Z. Ciunik, N. Kourkoumelis, M.A. Demertzis, Organotin mefenamic com-

plexes—preparations, spectroscopic studies and crystal structure of a triphenyltin ester of mefenamic acid: novel anti-tuberculosis agents, Applied organometallic chemistry 16.7 (2002) 360-368.

[10] F.A. Shah, S. Sabir, K. Fatima, S. Ali, I. Qadri, C Rizzoli, Organotin (IV) based anti-HCV drugs: synthesis, characterization and biochemical activity, Dalton Transactions 44.22 (2015) 10467-10478.

[11] J. Devi, S. Devi, A. Kumar, Synthesis, antibacterial evaluation and QSAR analysis of Schiff base complexes derived from [2, 2′-(ethylenedioxy) bis (ethylamine)] and aromatic aldehydes, MedChemComm 7.5 (2016) 932-947.

[12] J. Devi, S. Devi, A. Kumar, Synthesis, characterization, and quantitative structure–activity relationship studies of bioactive dehydroacetic acid and amino ether Schiff base complexes, Heteroatom Chemistry 27.6 (2016) 361-371.

[13] N. Zhang, Y. Tai, M. Li, P. Ma, J. Zhao, J Niu, Main group bismuth (III), gallium (III) and diorganotin (IV) complexes derived from bis (2-acetylpyrazine) thiocarbonohydrazone: synthesis, crystal structures and biological evaluation, Dalton Transactions 43.13 (2014) 5182-5189.

[14] X. Shang, X. Meng, E.C. Alegria, Q. Li, M.F.t.C. Guedes da Silva, M.L. Kuznetsov, A.J. Pombeiro, Syntheses, molecular structures, electrochemical behavior, theoretical study, and antitumor activities of organotin (IV) complexes containing 1-(4-chlorophenyl)-1-cyclopentanecarboxylato ligands, Inorganic Chemistry 50.17 (2011) 8158-8167.

[15] D. Tzimopoulos, I. Sanidas, A.-C. Varvogli, A. Czapik, M. Gdaniec, E. Nikolakaki, P.D Akrivos, On the bioreactivity of triorganotin aminobenzoates. Investigation of trialkyl and triarylyltin (IV) esters of 3-amino and 4-aminobenzoic acids, Journal of Inorganic Biochemistry 104.4 (2010) 423-430.

[16] M.-L. Sun, B.-F. Ruan, Q. Zhang, Z.-D. Liu, S.-L. Li, J.-Y. Wu, B.-K. Jin, J.-X. Yang, S.-Y. Zhang, Y.-P. Tian, Synthesis, crystal structures, electrochemical studies and anti-tumor activities of three polynuclear organotin (IV) carboxylates containing ferrocenyl moiety, Journal of Organometallic Chemistry 696.20 (2011) 3180-3185.

[17] N. Khan, Y. Farina, L.K. Mun, N.F. Rajab, N.J Awang, Syntheses, spectral characterization, X-ray studies and in vitro cytotoxic activities of triorganotin (IV) derivatives of p-substituted N-methylbenzylaminedithiocarbamates, Journal of Molecular Structure 1076 (2014) 403-410.

[18] C. Camacho-Camacho, I. Rojas-Oviedo, A. Garza-Ortiz, J. Cárdenas, R.A. Toscano, R. Gaviño, Synthesis, structural characterization and in vitro cytotoxic activity of novel polymeric triorganotin (IV) complexes of urocanic acid, Applied Organometallic Chemistry 27.1 (2013) 45-51.

[19] M. Khandani, T. Sedaghat, N. Erfani, M.R. Haghshenas, H.R. Khavasi, Synthesis, spectroscopic characterization, structural studies and antibacterial and antitumor activities of diorganotin complexes with 3-methoxysalicylaldehyde thiosemicarbazone, Journal of Molecular Structure 1037 (2013) 136-143.

[20] P. Rathelot, N. Azas, H. El-Kashef, F. Delmas, C. Di Giorgio, P. Timon-David, J. Maldonado, P. Vanelle, 1, 3-Diphenylpyrazoles: synthesis and antiparasitic activities of azomethine derivatives, European journal of medicinal chemistry 37.8 (2002) 671-679.

[21] M. Nath, P.K. Saini, A.J. Kumar, New di-and triorganotin (IV) complexes of tripodal Schiff base ligand containing three imidazole arms: Synthesis, structural characterization, anti-inflammatory activity and thermal studies, Journal of Organometallic Chemistry 695.9 (2010) 1353-1362.

[22] S.K. Hadjikakou, N. Hadjiliadis, Antiproliferative and anti-tumor activity of organotin compounds, Coordination Chemistry Reviews 253.1-2 (2009) 235-249.

[23] M.-X. Li, D. Zhang, L.-Z. Zhang, J.-Y. Niu, B.-S. Ji, Diorganotin (IV) complexes with 2-benzoylpyridine and 2-acetylpyrazine N (4)-phenylthiosemicarbazones: Synthesis, crystal structures and biological activities, Journal of Organometallic Chemistry 696.4 (2011) 852-858.

[24] J. Devi, S. Kumari, S. Devi, R. Malhotra, P. Kumar, B. Narasimhan, Synthesis, biological evaluation, and QSAR studies of organosilicon (IV) complexes derived from tridentate ONO Schiff bases of dehydroacetic acid and aromatic hydrazides, Monatshefte für Chemie-Chemical Monthly 146 (2015) 1995-2005.

[25] M.P. Scott, A twist in a hedgehog's tale, Nature 425.6960 (2003) 781-782.

[26] M. Jain, S. Gaur, V. Singh, R. Singh, Organosilicon (IV) and organotin (IV) complexes as biocides and nematicides: synthetic, spectroscopic and biological studies of N∩ N donor sulfonamide imine and its chelates, Applied organometallic chemistry 18.2 (2004) 73-82.

[27] S. Shujah, N. Muhammad, A. Shah, S. Ali, N. Khalid, A. Meetsma, Bioactive hepta-and penta-coordinated supramolecular diorganotin (IV) Schiff bases, Journal of Organometallic Chemistry 741 (2013) 59-66.

[28] S. Fani, B. Kamalidehghan, K.M. Lo, N.M. Hashim, K.M. Chow, F. Ahmadipour, development, therapy, Synthesis, structural characterization, and anticancer activity of a monobenzyltin compound against MCF-7 breast cancer cells, Drug design, development and therapy 9 (2015) 6191.

[29] M. Safari, M. Yousefi, H.A. Jenkins, M.B. Torbati, A. Amanzadeh, Synthesis, spectroscopic characterization, X-ray structure, and in vitro antitumor activities of new triorganotin (IV) complexes with sulfur donor ligand, Medicinal Chemistry Research 22 (2013) 5730-5738.

[30] H. Mansouri-Torshizi, M. Saeidifar, A. Divsalar, A. Saboury, Study on interaction of DNA from calf thymus with 1, 10-phenanthrolinehexyldithiocarbamatopalladium (II) nitrate as potential antitumor agent, Journal of Biomolecular Structure and Dynamics, 28 (2011) 805-814.

[31] T. Kondori, N. Akbarzadeh-T, K. Abdi, M. Dušek, V. Eigner, A novel cadmium (II) complex of bipyridine derivative: synthesis, X-ray crystal structure, DNA-binding and antibacterial activities, Journal of Biomolecular Structure and Dynamics, 38 (2020) 236-247.

[32] D. Sleep, J. Cameron, L.R. Evans, Albumin as a versatile platform for drug half-life extension, Biochimica et Biophysica Acta (BBA)-General Subjects, 1830 (2013) 5526-5534.

[33] M.S. Ali, H.A. Al-Lohedan, Spectroscopic and molecular docking investigation on the noncovalent interaction of lysozyme with saffron constituent “Safranal”, ACS omega, 5 (2020) 9131-9141.

[34] P. Alam, S.K. Chaturvedi, T. Anwar, M.K. Siddiqi, M.R. Ajmal, G. Badr, M.H. Mahmoud, R.H. Khan, Biophysical and molecular docking insight into the interaction of cytosine β-D arabinofuranoside with human serum albumin, Journal of Luminescence, 164 (2015) 123-130.

[35] Y.-J. Hu, Y. Liu, T.-Q. Sun, A.-M. Bai, J.-Q. Lü, Z.-B. Pi, Binding of anti-inflammatory drug cromolyn sodium to bovine serum albumin, International journal of biological macromolecules, 39 (2006) 280-285.

[36] M. Wang, Y. Yu, C. Liang, A. Lu, G. Zhang, Recent advances in developing small molecules targeting nucleic acid, International journal of molecular sciences, 17 (2016) 779.

[37] M.J. Fedor, J.R. Williamson, The catalytic diversity of RNAs, Nature reviews Molecular cell biology, 6 (2005) 399-412.

[38] R.L. Gurung, H.K. Lim, S. Venkatesan, P.S.W. Lee, M.P. Hande, Targeting DNA-PKcs and telomerase in brain tumour cells, Molecular cancer, 13 (2014) 1-14.

[39] A. Bottini, S.K. De, B. Wu, C. Tang, G. Varani, M. Pellecchia, Targeting influenza A virus RNA promoter, Chemical biology & drug design, 86 (2015) 663-673.

[40] L.-M. Tumir, I. Zonjić, K. Žuna, S.R. Brkanac, M. Jukić, A. Huđek, K. Durgo, I. Crnolatac, L. Glavaš-Obrovac, N. Cardullo, Synthesis, DNA/RNA-interaction and biological activity of benzo [k, l] xanthene lignans, Bioorganic Chemistry, 104 (2020) 104190.

[41] A.R. Simović, R. Masnikosa, I. Bratsos, E. Alessio, Chemistry and reactivity of ruthenium (II) complexes: DNA/protein binding mode and anticancer activity are related to the complex structure, Coord Chem Rev, 398 (2019) 113011.

[42] R. Palchaudhuri, P.J. Hergenrother, DNA as a target for anticancer compounds: methods to determine the mode of binding and the mechanism of action, Current opinion in biotechnology, 18 (2007) 497-503.

[43] M. Godzieba, S. Ciesielski, Natural DNA intercalators as promising therapeutics for cancer and infectious diseases, Current Cancer Drug Targets, 20 (2020) 19-32.

[44] Y. Suseela, N. Narayanaswamy, S. Pratihar, T. Govindaraju, Far-red fluorescent probes for canonical and non-canonical nucleic acid structures: current progress and future implications, Chemical Society Reviews, 47 (2018) 1098-1131.

[45] T. Hermann, E. Westhof, RNA as a drug target: chemical, modelling, and evolutionary tools, Current opinion in biotechnology, 9 (1998) 66-73.

[46] T. Hermann, Strategies for the design of drugs targeting RNA and RNA–protein complexes, Angewandte Chemie International Edition, 39 (2000) 1890-1904.

[47] N. Shahabadi, M. Mahdavi, B.Z. Momeni, Multispectroscopic analysis, atomic force microscopy, molecular docking and molecular dynamic simulation studies of the interaction between [SnMe2Cl2 (Me2phen)] complex and ct-DNA in the presence of glucose, Journal of Biomolecular Structure and Dynamics, 39 (2021) 5068-5082.

[48] S. Parveen, S. Jafri, H.Y. Khan, S. Tabassum, F. Arjmand, Elucidating the interaction of enantiomeric Cu (II) complexes with DNA, RNA and HSA: A comparative study, Polyhedron, 210 (2021) 115501.

[49] N. Bandyopadhyay, P. Basu, G.S. Kumar, B. Guhathakurta, P. Singh, J.P. Naskar, Biophysical studies on the interaction of a novel oxime based palladium (II) complex with DNA and RNA, Journal of Photochemistry and Photobiology B: Biology, 173 (2017) 560-570.

[50] Z. Zhou, X. Hu, G. Zhang, R. Wang, D. Gong, Exploring the binding interaction of Maillard reaction by-product 5-hydroxymethyl-2-furaldehyde with calf thymus DNA, Journal of the Science of Food and Agriculture, 99 (2019) 3192-3202.

[51] B.Z. Momeni, F. Haghshenas, S. Hadi, Synthesis, structural characterization and crystal structure of some dimethyltin complexes containing substituted 1, 10-phenanthroline, Journal of Molecular Structure 1142 (2017) 156-167.

[52] N. Shahabadi, B.Z. Momeni, S. Zendehcheshm, Studies on the interaction of [SnMe2Cl2 (bu2bpy)] complex with ct-DNA using multispectroscopic, atomic force microscopy (AFM) and molecular docking, Nucleosides, Nucleotides and Nucleic Acids, 38 (2019) 157-182.

[53] O. Trott, A.J. Olson, AutoDock Vina: improving the speed and accuracy of docking with a new scoring function, efficient optimization, and multithreading, Journal of computational chemistry 31.2 (2010) 455-461.

[54] X.-M. Dong, Y.-Y. Lou, K.-L. Zhou, J.-H. Shi, Exploration of association of telmisartan with calf thymus DNA using a series of spectroscopic methodologies and theoretical calculation, Journal of Molecular Liquids, 266 (2018) 1-9.

[55] S.U. Rehman, T. Sarwar, H.M. Ishqi, M.A. Husain, Z. Hasan, M. Tabish, Deciphering the interactions between chlorambucil and calf thymus DNA: a multi-spectroscopic and molecular docking study, Archives of biochemistry and biophysics, 566 (2015) 7-14.

[56] N. Shahabadi, F. Shiri, M. Norouzibazaz, A. Falah, Disquisition on the interaction of ibuprofen–Zn (II) complex with calf thymus DNA by spectroscopic techniques and the use of Hoechst 33258 and Methylene blue dyes as spectral probes, Nucleosides, Nucleotides and Nucleic Acids, 37 (2018) 125-146.

[57] E. Gratton, D.M. Jameson, G. Weber, B. Alpert, A model of dynamic quenching of fluorescence in globular proteins, Biophysical journal, 45 (1984) 789-794.

[58] M.R. Eftink, C.A. Ghiron, Fluorescence quenching studies with proteins, Analytical biochemistry, 114 (1981) 199-227.

[59] N. Shahabadi, F. Shiri, Multispectroscopic studies on the interaction of a copper (ii) complex of ibuprofen drug with calf thymus DNA, Nucleosides, Nucleotides and Nucleic Acids, 36 (2017) 83-106.

[60] N. Shahabadi, A. Akbari, F. Karampour, M. Falsafi, S. Zendehcheshm, In vitro cytotoxicity, antibacterial activity and HSA and ct-DNA interaction studies of chlorogenic acid loaded on γ-Fe2O3@ SiO2 as new nanoparticles, Journal of Biomolecular Structure and Dynamics, (2022) 1-21.

[61] N. Shahabadi, S. Zendehcheshm, F. Khademi, Selenium nanoparticles: Synthesis, in-vitro cytotoxicity, antioxidant activity and interaction studies with ct-DNA and HSA, HHb and Cyt c serum proteins, Biotechnology Reports, 30 (2021) e00615.

[62] N. Shahabadi, S. Zendehcheshm, F. Khademi, Green Synthesis, in vitro Cytotoxicity, Antioxidant Activity and Interaction Studies of CuO Nanoparticles with DNA, Serum Albumin, Hemoglobin and Lysozyme, ChemistrySelect, 7 (2022) e202202916.

[63] N. Shahabadi, S. Zendehcheshm, Evaluation of ct-DNA and HSA binding propensity of antibacterial drug chloroxine: multi-spectroscopic analysis, atomic force microscopy and docking simulation, Spectrochimica Acta Part A: Molecular and Biomolecular Spectroscopy, 230 (2020) 118042.

[64] D. Agudelo, P. Bourassa, M. Beauregard, G. Berube, H.-A. Tajmir-Riahi, tRNA binding to antitumor drug doxorubicin and its analogue, PLoS One, 8 (2013) e69248.

[65] J. Foresman, E. Frish, Exploring chemistry, Gaussian Inc., Pittsburg, USA, 21 (1996).

How to cite this manuscript: Nahid Shahabadi*, Saba Zendehcheshm, Badri Z Momeni, Fatemeh Khademi. Biomolecule (RNA) binding analysis of [$SnMe_2Cl_2(Me_2phen)$] complex: multi-spectroscopic analysis and docking simulation. Bioinorganic and Medicinal Inorganic Chemistry Journal, 1(1) 2023, 1-9. DOI: 10.22126/BMCJ.2023.2572